light passes to a lensless charge-coupled device (CCD) detector array. The reference beam is also expanded and passes to the CCD array which records the interference pattern of the object and reference beams. This single recording is essentially a digital Fourier transform hologram. To eliminate the need for a spatial carrier frequency, we record four versions of the hologram with the phase of the reference beam shifted by 0, $\pi/2$, π, and $3\pi/2$ radians, and in this manner we record complex valued holograms. Digital Fourier transformation of one of these holograms yields a standard angle-angle image of the object.

For HLR, the hologram recording procedure is repeated for a series of laser frequencies. As shown in Figure 1(a), the resulting data comprises a 3-D volume of Fourier data. The object's 3-D complex reflectivity is then recovered by digital inverse Fourier transformation of the data set. The resulting image occupies a 3-D array of complex-valued reflectivity values. There are a variety of ways to view the data. We typically transform the data set to a 2-D form by determining the range value where the maximum reflectivity occurs for each angular pixel. Figure 1(b) shows such a range encoded image. This image is a portion of President Lincoln's face taken from a penny. The depth interval between contours is roughly 8 μm and the total range extent of the image is 268 μm.

The resolution capabilities of HLR are dictated by several factors. First, the angular resolution is given by $\lambda R/D$, where R is the distance from the object to the detector array and D is the detector array width. Fine angular resolution can thus be obtained without the use of a lens. The range resolution of the system is given by $\lambda^2/(2\Delta\lambda)$ where $\Delta\lambda$ is the total bandwidth over which the laser is tuned. Thus broad tunability gives fine range resolution. By processing the phase of the 3-D image data, one can measure range with interferometric precision ultimately giving range resolution on the order of nanometers. One final feature of HLR imagery is that if the range extent of the object exceeds the unambiguous range of the system, the resulting image is wrapped in the range dimension, and for deep objects, range unwrapping must be performed.

REFERENCES

1. J.C. Marron and K.S. Schroeder, "Holographic laser radar," Opt. Lett. **18,** 1993, 385-387.
2. J.C. Marron and K.S. Schroeder, "Three-dimensional lensless imaging using laser frequency diversity," Appl. Opt. **31,** 1992, 255-262.

Free-space WDM Optical Mesh-connected Bus Interconnect

BY YAO LI, TING WANG, SATISH B. RAO, AND GEORGE Z. PAN, NEC RESEARCH INSTITUTE, PRINCETON, N.J., ADOLF W. LOHMANN, UNIVERSITY OF ERLANGEN-NURMBERG, GERMANY, TAO JIANG, THE CITY COLLEGE OF NEW YORK, NEW YORK, N.Y., AND JACOB SHARONY, COLUMBIA UNIVERSITY, NEW YORK, N.Y.

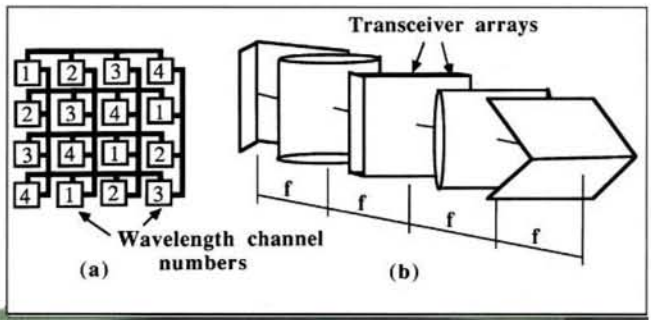

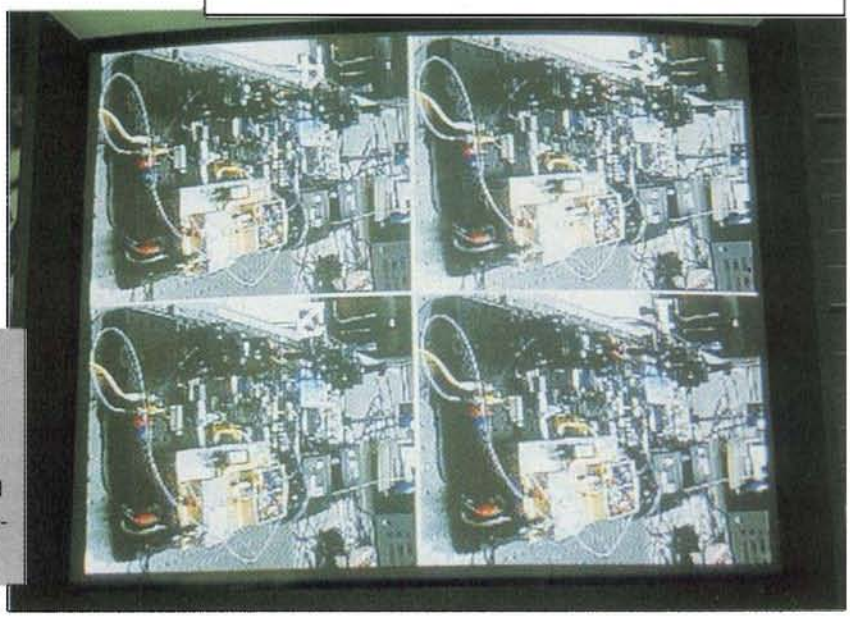

(c)

Have you ever wondered how the above-ground public transportation in a crowded urban area such as New York city is handled? The next time you visit "the Big Apple," note that most of the city buses follow routes along either east-west oriented streets or north-south oriented avenues in Manhattan. By taking three consecutive bus rides (turning corners twice), you can reach any desti-

Figure 1. **(a)** A schematic WDM-based MCB interconnecting 16 nodes with four different frequency channels; **(b)** a compact free-space WDM MCB layout using cylindrical optics for WDM bus array formations; and **(c)** video signal routing results of our three-stage optical demonstration prototype.

nation in this mesh-structured city. The concept behind this transportation pattern can be found in a communication network, commonly known as the Clos 3-stage network.[1] The mesh-connected bus (MCB) [2] topology is one way of laying out the Clos network in a 2D format (see Figure 1(a)). It has been shown that any permutation can be arranged, without experiencing internal blocking, in three global routing steps; permuting along the row buses, then along the column buses, and finally along the row buses.

Research leading to the implementation of a wavelength-division multiplexing (WDM) MCB free-space optical network is progressing at NEC Research Institute.[3] Compared to the existing single star-coupler-based WDM approaches in which each node experiences a power fan-out of N and a bandwidth capability of N wavelength channels, each WDM MCB node requires only a power fan-out of with a total required wavelength channels. The three hop routing speed compares favorably against $log_2 N$ hop multistage networks, such as the shuffle and the butterfly networks.[4] An additional feature here is that the MCB topology is suitable for a free-space optical implementation in the sense that each of the three required routings uses only one cylindrical optical component—a lens or a mirror. This is because cylindrical optics can convert a 2D dot pattern into an array of parallel lines each of which forms a WDM broadcast bus. Thus, a compact network architecture could probably take the form of Figure 1(b) in which the wavelength tuned transmitters and receivers are located on both sides of the middle block which is sandwiched between the perpendicularly oriented cylindrical lenses and right-angle reflectors.

With commercially available components, we have recently implemented an experimental prototype of the WDM MCB network to transmit 10 MHz multimedia signals formed by multiplexing video, stereo audio, and RS-232 data bands. Fixed-tuned lasers with output power of −5.2 dBm and with wavelengths around 1310 nm, and fiber Fabry-Perot type tunable filters and receivers with sensitivity of −31 dBm were used as transceivers. Some short fibers were used to link between the free-space bus routers and the transceivers. The power at each of the cylindrical lens-formed buses was enough to support 36 nodes with a signal-to-noise ratio better than 52 dB. The four quadrants of Figure 1(c) (our prototype) show the original camera picture and the pictures received at the outputs of stages 1 through 3, respectively. An overall signal-to-noise ratio of 49 dB was obtained at the last stage after the multimedia signals passed through three free-space routers and six supporting electric-to-optic or optic-to-electric conversion steps. The optical portion of the prototype, which has a power capability of supporting a total of $36^2 = 1296$ nodes, occupies no more than a 15×10 cm^2 area.

REFERENCES

1. C. Clos, "A study of non-blocking switching networks," Bell System Tech. J. **32**, 1953, 406-424.
2. L. D. Wittie, "Communication structure for large networks of microcomputers," IEEE Trans. Comput., C- **30**, 1981, 264-273.
3. Y. Li *et al.*, "Free-space mesh-connected bus networks using wavelength-division multiple access," Appl. Opt. **32**, 1993, in press.
4. K. Hwang, *Computer Architecture and Parallel Processing*, McGraw-Hill, New York, N.Y., 1984.

30 dB Contrast GaAlInAs Multiple Quantum Well Asymmetric Reflection Modulator at 1.3 μm

BY N. PEYGHAMBARIAN, T. OHTSUKI, G. KHITROVA, H.M. GIBBS, AND B.P. MCGINNIS, OPTICAL SCIENCES CENTER, UNIVERSITY OF ARIZONA, TUCSON, ARIZ., AND M.F. KROL AND R.K. BONCEK, ROME LABORATORY PHOTONICS CENTER, GRIFFISS AIR FORCE BASE, NEW YORK, N.Y.

High-speed optical communication interconnects and networks will require the use of high-contrast optical processing elements to fully use the bandwidth available in state-of-the-art optical fibers. Semiconductor quantum well modulators may be used for such applications. We have demonstrated[1,2] an all-optical GaAlInAs/AlInAs multipe quantum well (MQW) asymmetric reflection modulator for use at 1.3 μm with an on/off contrast ratio exceeding 1000:1 and an insertion loss of 2.2 dB at a pump intensity of 30 kW/cm^2, corresponding to a carrier density of 4.5×10^{17} cm^{-3}. The recovery time of the modulator is measured at ~ 725 psec, indicating that the operating speed of the device approaches 1 GHz.

Asymmetric reflection modulators consist of an asymmetric Fabry-Perot étalon formed by an optically nonlinear spacer between a low reflectivity front mirror and high reflectivity back mirror. Our asymmetric reflection modulator consists of a 65 period 69 Å $Ga_{0.376}Al_{0.094}In_{0.53}As$ well/89 Å $Al_{0.48}In_{0.52}As$ barrier MQW nonlinear spacer on top of a 24 period 936Å $Ga_{0.3}Al_{0.18}In_{0.52}As$/1003Å $Al_{0.48}In_{0.52}As$ quarter-wave stack back mirror. This structure was grown lattice-matched on a semi-insulating InP substrate by molecular beam epitaxy. The etalon front mirror is formed by the air/spacer interface with a reflectance of $R_f \approx 0.31$, and the quarter-wave stack back mirror has a reflectance of $R_b \approx 0.92$. The total spacer thickness was L = 1.027 μm. The modulator was designed such that the Fabry-Perot resonance is located on the long wavelength side of the heavy-hole exciton peak to take advantage of pump-beam induced, large absorptive and refractive nonlinearities. In the absence of the pump, the absorption near the heavy-hole exciton is high, resulting in a balanced cavity and near-zero reflectance at resonance. When the pump is present, the photogenerated electron and hole populations saturate the absorption near the heavy-hole exciton and result in an increase in the reflectance at resonance by unbalancing the Fabry-Perot cavity. A considerable shift occurs in the Fabry-Perot resonance due to the change in refractive index related by the Kramers-Kronig transformations to the pump-induced absorption change.

The nonlinear reflectance spectra at pump intensities of 0.0, 6.6, and 41 kW/cm^2 are shown in the figure (next page). The reflectance rapidly increases from a value of 0.00055 ± 0.0008 at zero pump intensity to a value approaching 0.72 as